

## Time-resolved reflectivity measurements on a plasma mirror with few-cycle laser pulses

Yutaka Nomura<sup>1,4</sup>, László Veisz<sup>1</sup>, Karl Schmid<sup>1,2</sup>,  
Tibor Wittmann<sup>1</sup>, Johannes Wild<sup>3</sup> and Ferenc Krausz<sup>1,2,3</sup>

<sup>1</sup> Max-Planck-Institut für Quantenoptik, D-85748 Garching, Germany

<sup>2</sup> Lehrstuhl für Experimentalphysik, Department für Physik,

Ludwig-Maximilians-Universität München, D-85748 Garching, Germany

<sup>3</sup> Institut für Photonik, Technische Universität Wien, A-1040 Wien, Austria

E-mail: [yutaka.nomura@mpq.mpg.de](mailto:yutaka.nomura@mpq.mpg.de) and [laszlo.veisz@mpq.mpg.de](mailto:laszlo.veisz@mpq.mpg.de)

*New Journal of Physics* **9** (2007) 9

Received 13 October 2006

Published 18 January 2007

Online at <http://www.njp.org/>

doi:10.1088/1367-2630/9/1/009

**Abstract.** We present time-resolved reflectivity measurements on a plasma mirror and demonstrate the contrast improvement of sub-10-fs pulses. Detailed characterization of the spatial peak and the average reflectivity, the spatial and temporal properties of the reflected pulses for  $p$ - and also for  $s$ -polarization are discussed. A complete third-order correlation is measured to compare the temporal structures of the pulses before and after the plasma mirror. Simulation of the hydrodynamic expansion of the plasma supports the measured pulse properties after the reflection.

The advent of laser systems with extremely high intensity [1]–[3] has opened a new regime of laser–solid interaction. Very high intensity contrast is needed for such laser pulses, because the prepulses or pedestal can be otherwise intense enough to generate plasma before the main peak arrives. In such cases, due to the hydrodynamic expansion of the plasma, the main pulse does not interact with a steep electron density gradient. This effect is unfavourable for many applications such as high-order harmonic generation on a solid surface [4, 5] and ion acceleration [6].

Various methods have been tested to improve the contrast such as Sagnac interferometer [7], nonlinear elliptic polarization rotation in air [8], and cross-polarized wave generation in a crystal [9]. The drawbacks of these techniques are their low-energy throughput and the limited applicable input energy. The plasma mirror [10], on the other hand, provides pulse cleaning with

<sup>4</sup> Author to whom any correspondence should be addressed.

higher throughput without limitation on the input energy [2]. In this method, the pulses are sent on to a transparent target. While the prepulses/pedestal are transmitted, the main peak is so intense that its leading edge ionizes the target and forms a plasma on the target surface. This plasma then reflects the remaining part of the incident pulse. This way the contrast between the leading part of the pedestal or prepulses and the main pulse can be improved significantly in the reflected beam. Several investigations have been performed to study the reflectivity of the plasma mirror [11] and the reflected beam profile [12]–[14]. To reach even better contrast improvement a double plasma mirror pulse cleaner has been tested [14]. Although intense few-cycle pulses with a sufficiently high contrast will open up new prospects for many applications [15, 16], the previous experimental studies were done using pulses with 25 fs duration or longer and no experiment has been done in the sub-10-fs regime. Previous time-dependent reflectivity studies resulted in 200–1000 fs rise time [17]–[19] for the formation of a reflecting plasma surface with 60 fs or longer pulse durations.

In this paper, we report on the performance of a plasma mirror with 7 fs incident pulses. The reflectivity of the plasma mirror is measured for both  $p$ - and  $s$ -polarization at  $45^\circ$  angle of incidence, and the reflected pulses are characterized both spatially and temporally. A complete high dynamic range third-order correlation of the reflected pulses, which allows us to obtain the time-resolved reflectivity of the plasma mirror, are presented for the first time to the best of our knowledge.

The experiment was carried out with a broadband Ti:sapphire laser system based on chirped-pulse amplification with three multi-pass amplifier stages and a hollow-fibre compressor [20]. The system typically delivered pulses with 550  $\mu\text{J}$  energy and 7 fs duration at the central wavelength of 730 nm—the spectrum extended from 550 to 900 nm—at 1 kHz repetition rate. The output beam was guided through a vacuum beamline to the target chamber. The energy on the target was  $\sim 350$ – $400 \mu\text{J}$ .

The experimental set-up is shown in figure 1. The polarization of the incident beam could be swapped between  $p$  and  $s$  before entering into the target chamber. The beam with 50 mm diameter was focused on to a glass target with an  $f = 150$  mm,  $90^\circ$  silver off-axis parabola ( $F/3$ ). Three motorized stages allowed to rotate the target and translate it parallel to the surface and parallel to the incident beam ( $z$ -direction). At 1 kHz repetition rate a target lasted approximately for an hour. The reflected beam from the target was refocused with a thin achromatic lens and sent to a detector outside the vacuum chamber. We measured the reflected energy, the beam profile around the focus of the incident and the reflected beam, the spatial peak reflectivity, and the temporal structure with high dynamics of the incident and also of the reflected pulses.

We characterized the efficiency of the plasma mirror by measuring the spatial-integral or ‘average reflectivity’ and the ‘peak reflectivity.’ The average reflectivity is given by the ratio of the reflected energy to the incident energy. We calculate the peak reflectivity as the ratio of the peak fluences, which are obtained from the measured beam profiles on the target and the incident energy. As we will see, this gives the same as the ratio of the peak intensities, which is the definition of the reflectivity. Figure 2(a) shows the average reflectivity for  $p$ -polarization as a function of the average incident fluence, which is determined with respect to the spatial full width at half maximum (FWHM) area of the focused beam. The energy measured with the power meter was averaged over some thousand shots. The incident fluence was changed by either moving the target out of focus ( $z$ -scan) or decreasing the energy of the incident pulse (energy scan). Different sets of measurements are shown with different symbols in figure 2. The measurements were well reproducible and gave the same results for  $z$ -scan and for energy scan.

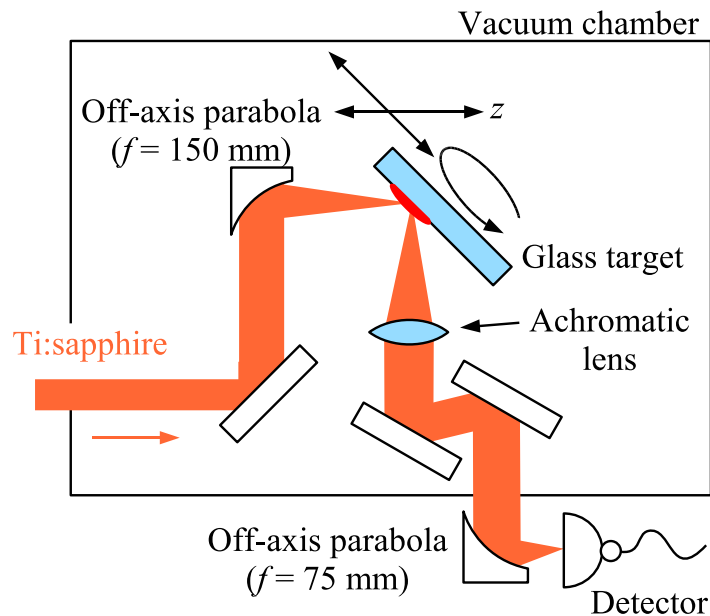


**Figure 1.** Schematic of the experimental set-up.

The highest average reflectivity reached up to  $\sim 40\%$ , whereas the lowest reflectivity was as low as  $\sim 0.5\%$  because the incidence angle ( $45^\circ$ ) was close to Brewster's angle ( $\sim 56^\circ$ ). From these values, a contrast improvement of two orders of magnitude is expected. We also measured the average reflectivity with longer pulse durations, which was achieved by either chirping the pulse or clipping the spectrum. The pulse duration was increased up to 60 fs, i.e., a factor of 9, but no significant change was observed in the behaviour of the reflectivity versus fluence dependence. Therefore, we plotted the reflectivity as a function of the incident fluence in figure 2.

The average reflectivity measured for *s*-polarization is plotted in figure 2(b). Although the highest reflectivity reached up to  $\sim 65\%$ , the expected contrast improvement is only one order of magnitude due to the relatively high Fresnel reflectivity at *s*-polarization, which is 7.6% at  $45^\circ$  angle of incidence for our target material. The results plotted in figure 2(b) had larger fluctuations than those in figure 2(a) due to the different laser conditions. Reducing the reflectivity with anti-reflection (AR) coated targets can boost the contrast improvement up to factor of 200 [12]. Therefore, using *s*-polarized beam with AR-coated targets is ideal for obtaining the maximal throughput (65%). On the other hand, AR-coated targets are expensive, especially when they have to be replaced frequently. Using *p*-polarized light solves this problem at the cost of decreased throughput (40%). The contrast improvement factors are in the same order for *s*-polarized light with AR-coated targets and for *p*-polarized light with ordinary targets, at  $45^\circ$  incidence angle. Using Brewster's angle increases the improvement factor for *p*-polarization even more, although the alignment is more complicated. The spatial peak reflectivity for *p*-polarized pulses is depicted in figure 2(c) as a function of the peak fluence. The maximum value was above 60%.

The spectra of the incident and reflected pulses were also measured, but they were almost identical and no significant blue shift was observed.

To investigate the spatial characteristics of the reflected beam, we collimated it with an achromatic lens ( $f = 150$  mm) and refocused with an  $f = 75$  mm off-axis parabola. The image of the refocused spot was magnified with a microscope objective and captured by a charge-coupled

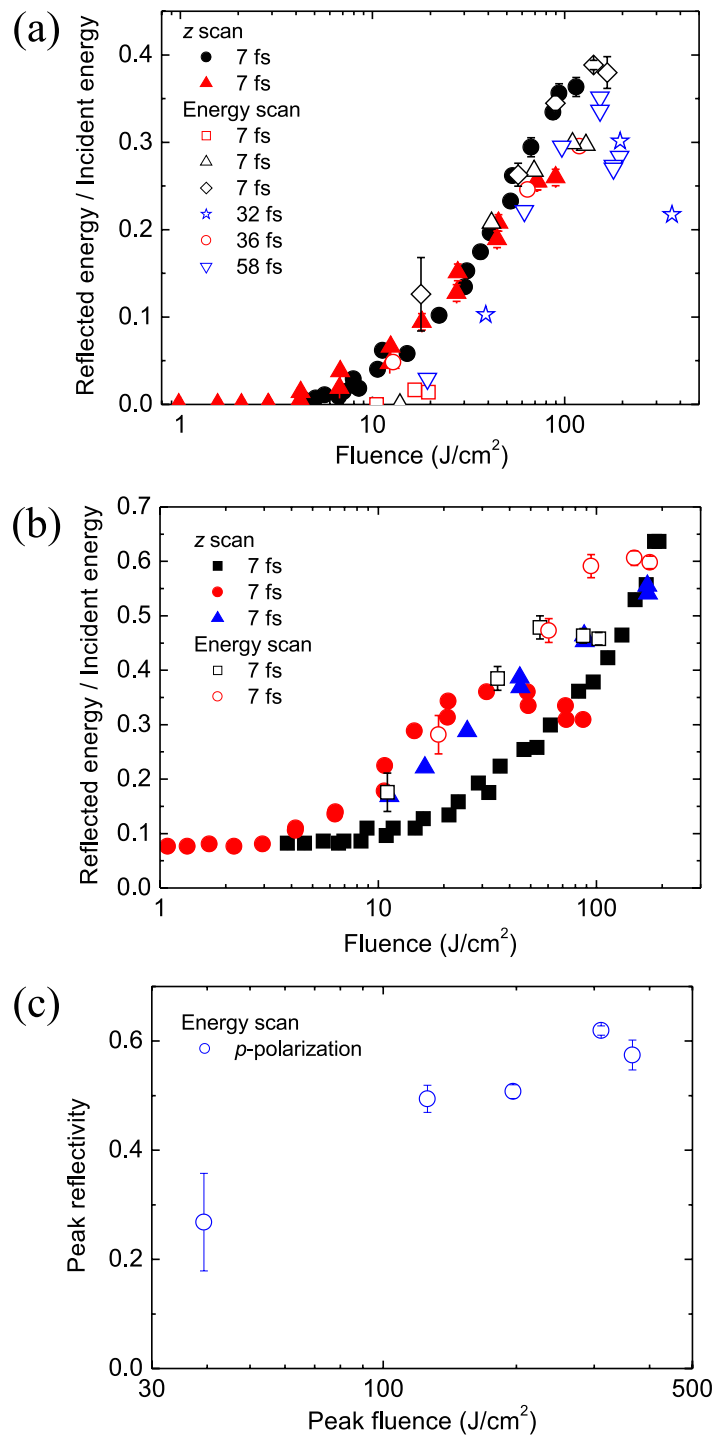


**Figure 2.** Average reflectivity of the plasma mirror for (a) *p*-polarization and (b) *s*-polarization as a function of the average incident fluence. Different symbols represent different sets of measurements. For *p*-polarization, the highest and lowest reflectivity measured are  $\sim 40\%$  and  $\sim 0.5\%$ , respectively, therefore a contrast improvement of two orders of magnitude is expected. (c) Spatial peak reflectivity for *p*-polarized beam plotted against the spatial peak incident fluence.

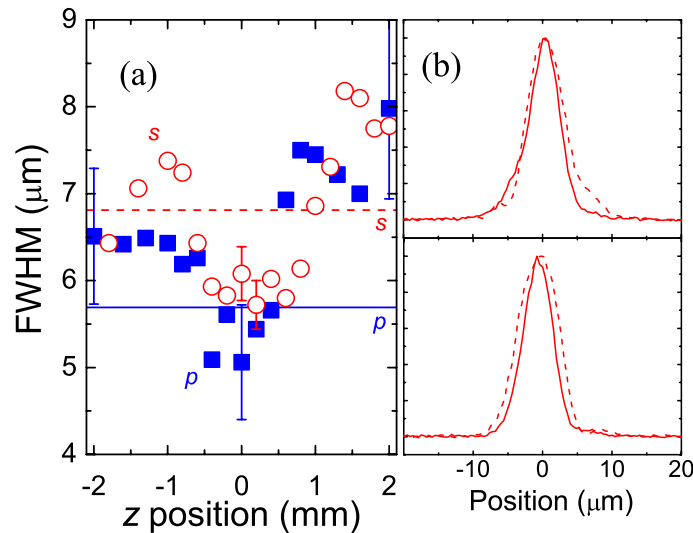


**Figure 3.** (a) Refocused spot size (FWHM) as a function of the plasma-mirror position in the focal ( $z$ ) direction. The polarization of the incident beam was  $p$  (solid square) or  $s$  (open circle). Horizontal lines indicate the reference spot size without activating the plasma mirror for  $p$  (solid) and  $s$  (dashed) polarization. (b) Horizontal and vertical lineouts of the refocused beam profile with the target in the focus ( $z = 0$ ) for  $s$ -polarization with (solid) and without (dashed) plasma mirror.

device beam profiler. The target was moved in the focal ( $z$ ) direction and the imaging system was adjusted for each measurement. The measured spot diameters are plotted in figure 3(a). The horizontal lines indicate the spot diameter without activating the plasma mirror, i.e., with low input energy. The different focus diameters for  $s$ - and  $p$ -polarizations are due to different alignments of the beam line. A horizontal and a vertical lineout of the refocused beam profile are plotted for  $s$ -polarization with (solid) and without (dashed) plasma mirror in figure 3(b) when the target was in the focus ( $z = 0$ ). We observed two effects on the reflected beam: cleaner beam profile and smaller refocused spot. Both changes can be explained by the fluence-dependent reflectivity of the plasma mirror. The plasma mirror reflects more efficiently at the central part of the beam, while the reflection at the surrounding area is relatively suppressed, which acts as a spatial filter resulting in a cleaner beam profile [21]. At the same time, this fluence-dependent reflectivity makes the peak narrower, which results in a smaller spot size on the plasma mirror and consequently a smaller refocused spot size.

We also investigated the temporal characteristics of the reflected beam by measuring a high dynamic range third-order correlation. The polarization of the beam incident to the target was set to  $p$  because a better contrast improvement was expected. The fluence on the plasma mirror was estimated to be  $\sim 60 \text{ J cm}^{-2}$ . The reflected beam was recollimated and sent into a home-made third-order correlator [22]. Figure 4 shows the measured third-order correlation of the reflected pulse together with that of the incident pulse. The negative delay represents the leading edge of the pulse. Although the measured contrast was limited by the low energy ( $\sim 50 \mu\text{J}$ ) sent into the correlator, the expected contrast improvement of two orders of magnitude at the pulse front is striking, for example, around  $-2$  or at  $-8.5$  ps. The peak appearing at  $-1.5$  ps is an artefact

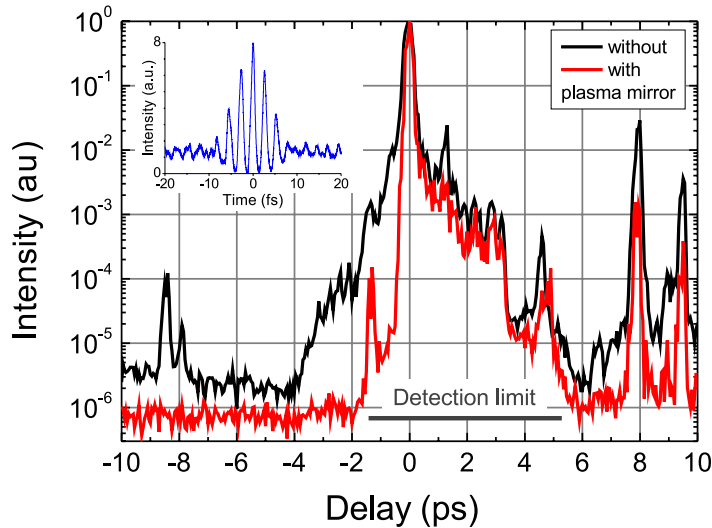


**Figure 4.** Third-order correlation measured with (red) and without (black) the plasma mirror. Negative delay represents the leading edge of the pulse. Although the measured contrast was limited by the low input energy ( $\sim 50 \mu\text{J}$ ), contrast improvement of two orders of magnitude is seen in the leading edge, for example, around  $-2$  ps. The inset shows a second-order interferometric correlation of the 6–7 fs input pulse.

from a post pulse, which appears due to the nature of correlation measurements. Also a pulse-steepening effect is evident on the rising edge [23]. On the other hand, no effect is observed on the falling edge of the pulse. Figure 4 also indicates that the plasma is generated 400–500 fs before the main pulse arrives. Therefore, the plasma mirror is efficiently generated with the pedestal of our sub-10-fs pulses, similarly to the previous experiments with longer pulses. It is apparent that the reflectivity is constant during the pulse, hence the way we attained the peak reflectivity using the fluences is correct. Since  $100 \mu\text{m}$  thick crystals were used in the correlator to gain a stronger signal, the third-order correlation does not reflect the short pulse duration. A second-order interferometric correlation trace in the inset of figure 4 shows the 6–7 fs duration of the incident pulses.

Figure 5 depicts the time-resolved reflectivity of the plasma mirror for  $p$ -polarization obtained by dividing the correlation of the reflected pulse by that of the incident pulse. We normalized the curve by setting the average reflectivity between 0 and 4 ps to the expected peak reflectivity of 50%. A step rise in the reflectivity is clearly seen at  $-500$  fs. This step rise indicates that the plasma is generated  $\sim 500$  fs before the main pulse. We also see a decrease in the reflectivity  $\sim 6$  ps after the main pulse.

To further understand the physical process, we simulated the hydrodynamic expansion of the plasma with the simulation code MEDUSA [24]. As the input pulse, we used a 7 fs Gaussian pulse sitting on 1.7 ps Gaussian pedestal with  $2 \times 10^{-4}$  contrast and 7 fs Gaussian prepulse 8.5 ps before the main peak with  $10^{-4}$  contrast. The parameter was determined by the fit on the third-order correlation without the plasma mirror. The simulation shows that the scale length  $L \equiv n_e/|dn_e/dz|$  of the plasma, where  $n_e$  is the electron density, is  $\sim 0.03\lambda$  at the critical density when the main peak of the pulse arrives. If the scale length is too large, a plasma mirror acts

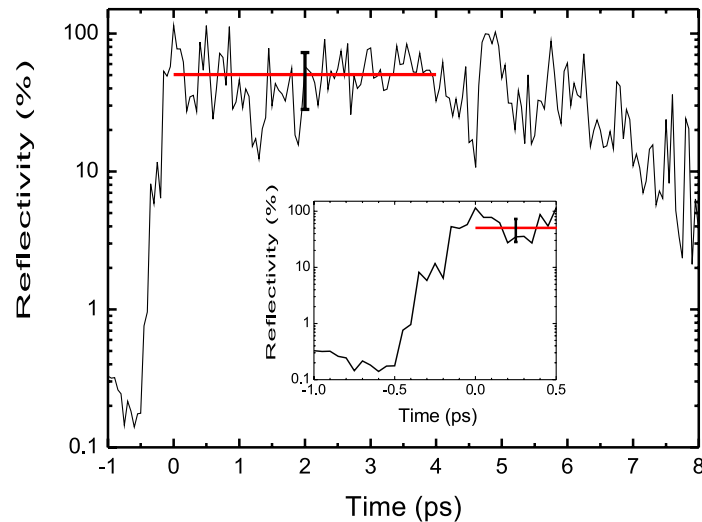


**Figure 5.** Time-resolved peak reflectivity of the plasma mirror calculated from the correlations in figure 4. The horizontal red line is the average value of the reflectivity between 0 and 4 ps and the error bar corresponds to the standard deviation. Inset: the fast increase of the reflectivity at the leading edge.

similarly to a chirped mirror because different wavelengths are reflected at different depths in the plasma surface due to different critical densities. With this scale length, however, this chirping effect is negligible and the pulse duration stays the same after the plasma mirror. The simulation also shows that the scale length exceeds  $0.1\lambda$  around +4 ps after the main peak. Above this scale length resonant absorption [25] takes place and reaches 60–80% at  $45^\circ$  incidence angle, which explains the decrease of the reflectivity around 6 ps.

It is worth investigating whether the plasma mirror works with sub-10-fs pulses with the higher contrast. For example, applying another plasma mirror to the pulse cleaned by the first plasma mirror, which will lead to the contrast improvement of more than four orders of magnitude. Since the energy in the pedestal is much lower, the pedestal may not trigger the plasma mirror any more. What the plasma mirror does to the pulse in this case is an open question.

In conclusion, we have demonstrated the contrast improvement of sub-10-fs pulses by a plasma mirror. The reflected pulses were spatially and temporally cleaned while the spatial peak reflectivity for *p*-polarization reached  $\geq 60\%$  and the average reflectivity had a value of  $\sim 65\%$  ( $\sim 40\%$ ) for *s*- (*p*-) polarization at  $45^\circ$  angle of incidence. The first measurement of the complete high-dynamic correlation revealed the temporal structure of the pulses reflected from the plasma mirror. The time-resolved reflectivity of the plasma mirror was determined with the help of these results, showing the contrast improvement of two orders of magnitude and the pulse steepening at the leading edge. Improving the contrast with the plasma mirror will lead to better performances in experiments such as high-order harmonic generation on plasma surfaces and ion acceleration.

## Acknowledgments

The authors appreciate contributions from J Seres and E Seres. This study was supported by the Austrian Science Foundation. L Veisz acknowledges support from a Lise Meitner fellowship

under the project number M714-N08. This research was sponsored by FWF, Austria, through the grant Z63.

## References

- [1] Strickland D and Mourou G 1985 *Opt. Commun.* **56** 219
- [2] Perry M D *et al* 1999 *Opt. Lett.* **24** 160
- [3] Dromey B *et al* 2006 *Nature Phys.* **2** 456
- [4] Zepf M *et al* 1998 *Phys. Rev. E* **58** R5253
- [5] Monot P, Doumy G, Dobosz S, Perdrix M, D'Oliveira P, Quéré, Réau F and Martin P 2004 *Opt. Lett.* **29** 893
- [6] Hegelich B M, Albright B J, Cobble J, Flippo K, Letzring S, Paffett M, Ruhl H, Schreiber J, Schulze R K and Fernández J C 2006 *Nature* **439** 441
- [7] Renault A, Augé-Rochereau F, Planchon T, D'Oliveira P, Auguste T, Chériaux G and Chambaret J P 2005 *Opt. Commun.* **248** 535
- [8] Jullien A, Augé-Rochereau F, Chériaux G, Chambaret J P, D'Oliveira P, Auguste T and Falcoz F 2004 *Opt. Lett.* **29** 2184
- [9] Minkovski N, Petrov G I, Saltiel S M, Albert O and Etchepare J 2004 *J. Opt. Soc. Am. B* **21** 1659
- [10] Kapteyn H C, Murnane M M, Szoke A and Falcone R W 1991 *Opt. Lett.* **16** 490
- [11] Ziener C, Foster P S, Divall E J, Hooker C J, Hutchinson M H R, Langley A J and Neely D 2003 *J. Appl. Phys.* **93** 768
- [12] Doumy G, Quéré F, Gobert O, Perdrix M, Martin P, Audebert P, Gauthier J C, Geindre J P and Wittmann T 2004 *Phys. Rev. E* **69** 026402
- [13] Dromey B, Kar S, Zepf M and Foster P 2004 *Rev. Sci. Instrum.* **75** 645
- [14] Wittmann T, Geindre J P, Audebert P, Marjoribanks R S, Rousseau J P, Burgy F, Douillet D, Lefrou T, Ta Phuoc K and Chambaret J P 2006 *Rev. Sci. Instrum.* **77** 083109
- [15] Tsakiris G D, Eidmann K, Meyer-ter-Vehn J and Krausz F 2006 *New J. Phys.* **8** 19
- [16] Geissler M, Schreiber J and Meyer-ter-Vehn J 2006 *New J. Phys.* **8** 186
- [17] Grimes M K, Rundquist A R, Lee Y S and Downer M C 1999 *Phys. Rev. Lett.* **82** 4010
- [18] Bor Z, Racz B, Szabo G, Xenakis D, Kalpouzos C and Fotakis C 1995 *Appl. Phys. A* **60** 365
- [19] von der Linde D, Sokolowski-Tinten K and Bialkowski J 1997 *Appl. Surf. Sci.* **109/110** 1
- [20] Verhoef A J, Seres J, Schmid K, Nomura Y, Tempea G, Veisz L and Krausz F 2006 *Appl. Phys. B* **82** 513
- [21] Moncur N K 1977 *Appl. Opt.* **16** 1449
- [22] Tavella F, Schmid K, Ishii N, Marcinkevičius A, Veisz L and Krausz F 2005 *Appl. Phys. B* **81** 753
- [23] Hentschel M, Uemura S, Cheng Z, Sartania S, Tempea G, Spielmann C and Krausz F 1999 *Appl. Phys. B* **68** 145
- [24] Christiansen J P, Ashby D E T F and Roberts K V 1974 *Comput. Phys. Commun.* **7** 271
- [25] Gibbon P 2005 *Short Pulse Laser Interactions with Matter* (London: Imperial College Press)